Lawrence Berkeley Laboratory
UNIVERSITY OF CALIFORNIA

Accelerator & Fusion Research Division

Submitted to Nuclear Fusion

CHARACTERISTICS OF THE BERKELEY MULTI-CUSP ION SOURCE

K. W. Ehlers and K. N. Leung

May 1979

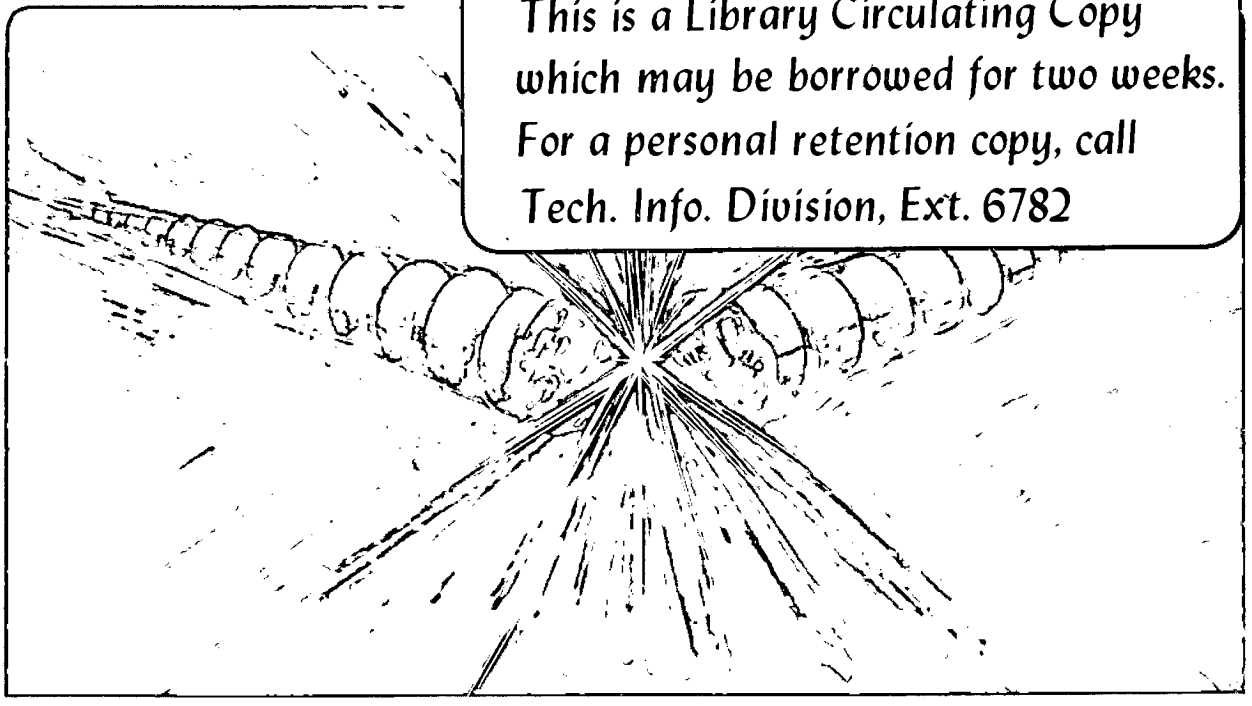

Prepared for the U. S. Department of Energy
under Contract W-7405-ENG-48

DISCLAIMER

CHARACTERISTICS OF THE BERKELEY MULTI-CUSP ION SOURCE

K. W. Ehlers and K. N. Leung

Lawrence Berkeley Laboratory
University of California
Berkeley, California 94702

May 1, 1979

ABSTRACT

The performance of a cubical permanent magnet generated line-cusp ion source has been investigated for use with neutral beam injectors. This source has been operated with discharge currents greater than 500 A and ion current densities higher than 400 mA/cm^2 at the extraction grid. The uniformity of the density profile across the extraction area is found to be dependent on the gas pressure. By using a fast Langmuir probe sweeping circuit, the electron temperature and the plasma density and potential have been analyzed for different discharge powers and gas pressures. The heat load on the plasma grid when it is electrically floating or connected to the negative cathode has been compared calorimetrically. The use of lanthanum hexaboride and impregnated oxide cathodes have been investigated for the purpose of long pulse operation. The phenomenon of mode flipping is found to occur quite frequently during a discharge with these magnetic-field-free cathodes. Species composition as a function of discharge power and chamber length is measured by a mass spectrometer.

I. INTRODUCTION

Neutral beam injection has proved to be a successful heating method for tokamaks as well as for mirror machines. Recently, a record high fivefold increase of ion temperature in PLT at Princeton has been achieved by 2 MW of injected power [1]. For future fusion devices, such as TFTR, Doublet III, MFTF and JET, plasma heating will depend heavily on high-power neutral beams. For this purpose, the ion source for the injector should be capable of generating a dense, uniform and quiescent plasma with a high percentage of atomic species. The permanent magnet generated line-cusp type plasma source developed at UCLA [2] is able to fulfill most of these requirements, and it has already been used as a neutral beam ion source at Culham and ORNL [3,4].

At Berkeley, the performance of a cubical multiline-cusp ion source has been studied for the development of the TFTR neutral beam injector. This source has been operated with discharge current greater than 500 A to generate hydrogen or deuterium ion beams with current density higher than 400 mA/cm^2 at the extraction grid. The uniformity of the density profile across the extraction area is found to be dependent on the neutral gas pressure. By using a fast Langmuir probe sweeping circuit, the electron temperature and the density and potential of the plasma have been analyzed for different discharge powers and gas pressures. The source can be operated with the plasma grid floating or connected to the negative cathode. The heat load on the plasma grid for these two modes of operation has been compared calorimetrically.

During the source operation, several types of discharge modes have been observed. The mechanism for this mode switching is found to be closely related to the geometry and temperature of the cathode and to the area of the anode. For the purpose of longer pulse operation ($\sim$1.5 sec), new types of cathode (such as LaB_6 and impregnated oxide emitters) other than tungsten filaments are being investigated. Ion species composition as a function of discharge power and the length of the source chamber has also been studied by a mass spectrometer.

II. EXPERIMENTAL APPARATUS

Figure 1 shows a schematic diagram of the ion source which is a 0.64 cm thick, water-cooled, cubical copper chamber with each side 24 cm in length. One end of the chamber is enclosed by a copper grid which simulates the plasma grid of a standard extraction system. This grid is isolated from the source chamber by a sheet of machineable glass ceramic. It is also partly covered by quartz insulator in order to avoid electrical breakdown to the chamber during the discharge. Groves are milled on the external wall so that samarium-cobalt magnets ($B_{max} \cong 4$ kG) are mounted within 0.32 cm from the vacuum. These magnets are arranged in a continuous line-cusp configuration (cusp spacing $\cong$ 4 cm) to generate a surface magnetic field for primary electron as well as for plasma confinement [5]. Since the chamber has a square cross-section, two types of magnet geometries can be employed. In the arrangement shown in Fig. 2A, a line cusp exists at each corner of the chamber, resulting a uniform density profile in the diagonal direction. In the arrangement of Fig. 2B, the magnet columns are removed from the corners. Because the corner regions are now protected by the magnetic field, the loss of plasma to the chamber will be reduced. However, this geometry may not produce a uniform diagonal profile across the extraction area because the density drops off at a considerable distance from two of the corners. All the data presented in the following sections are obtained by using the geometry of Fig. 2A.

Deuterium or hydrogen gas is introduced into the source chamber through a pulsed valve just before the discharge or arc voltage is switched on. The plasma is produced by primary ionizing electrons emitted from eight, 0.15 cm-diam tungsten filaments, which are normally biased at 60-80 V with respect to the chamber

wall (the anode). These filaments are located approximately 7 cm from the back wall and they are mounted on molybdenum holders. The heater current for each filament normally exceeds 120 A which is sufficient to generate a magnetic field as high as 300 G on the filament surface. Each filament of the source has several bends. This arrangement will enable the thermal electrons to leave the filament after drifting (the E x B and grad B drifts) a short distance and so will reduce the loss of electrons to the positive filament holder [6]. When spring-shape, non-inductive filaments or cylindrical lanthanum hexaboride or impregnated oxide cathodes are being used, the switching from one discharge mode to another occurs quite frequently during the source operation. This phenomenon of mode-flipping is described in more detail in Section V. The density, potential, and electron temperature of the source plasma are obtained from the Langmuir probe measurements.

III. PLASMA GRID BIAS VOLTAGE

The multiline-cusp ion source is relatively simple to operate. There are three main components in the source; the filaments (cathode), the chamber (anode), and the plasma grid. Since the grid is electrically isolated from the chamber, its voltage relative to the anode or cathode can be easily varied. In order to achieve the best efficiency, the grid should be biased negatively with respect to the anode. It has been shown that the plasma density at the center of the source chamber and the ion current collected by the plasma grid I_g becomes saturated when the grid bias voltage V_g is greater than the discharge (arc) voltage V_d [7]. In order to avoid the use of a separate power supply for biasing the grid, the source can be operated conveniently either with the grid electrically floating or by connecting it to the negative terminal of the filament as shown in the circuit diagram of Fig. 3. In the latter arrangement, the current passing through the discharge power supply I_d is the sum of the discharge current I_a and the grid return current I_g. With the grid floating, those electrons with perpendicular energy less than the floating potential will be reflected back. However, when the grid is connected to the negative terminal of the filament ($V_g = V_d$), the majority of the primary electrons will be reflected. As a result, a higher ion production rate is achieved. Indeed Fig. 3 shows that with $V_d = 70$ V, the deuterium ion current density J_i (measured by a Langmuir probe located approximately 2 mm from the grid) is in general 12% higher when the grid is connected to the negative terminal of the filament. If the grid return current I_g is not included in I_d, then the percentage increase becomes 28%

The heat load on the plasma grid for these two modes of operation has also been compared calorimetrically. The grid is cooled by water circulating around the outer edge. The difference in the inlet and outlet water temperature is converted by two YSI thermistors into a voltage signal which is then recorded on a Norland 2001-A computation system as shown in Fig. 4 [8]. The four peaks show how the grid is heated up during four consecutive discharge pulses after the source has reached an equilibrium state. The area under the trace (which can be computed by the Norland system) is proportional to the amount of heat dissipated on the grid for the four discharge pulses. Measurements have been taken in a deuterium plasma for the case when the grid is floating and when it is connected to the negative cathode. The results are summarized in Table I.

Although the filament heater current and the neutral gas pressure are the same for both modes of operation, the discharge power P_d is found to be about 5.8% higher when the grid is floating. Approximately the same percentage increase is also observed in the heat loading P_h on the plasma grid. Thus the power dissipated on the grid depends mostly on the total discharge power of the source.

Results of this calorimetry measurement can also provide information on the amount of primary and background electrons collected by the plasma grid when it is floating. If the grid is connected to the negative cathode, it collects essentially ion current. In this case, the power density dissipated by the ions on the grid $P_t = J_i V_d$, where J_i is the ion current density at the grid. When the grid is floating, ions as well as primary and background electrons are collected. The total power density dissipated on the grid is given by:

$$P_f = J_i(V_d - V_{float}) + J_p V_{float} + P_e \qquad (1)$$

where V_{float} is the potential of the grid relative to the cathode, J_p is the primary electron current density and P_e is the power density dissipated by the background electrons on the grid. If z is the axial direction of the source, then

$$P_e = \int_{-\infty}^{\infty} dv_x \int_{-\infty}^{\infty} dv_y \int_{v_{zo}}^{\infty} [\tfrac{1}{2} m(v_x^2 + v_y^2 + v_z^2) - eV]\, v_z\, f(v_x, v_y, v_z)\, dv_z \qquad (2)$$

where $v_{zo} = (2eV/m)^{1/2}$, $V = V_d - V_{float}$, $f(v_x, v_y, v_z)$ is the electron distribution function, and m and e are the electron mass and charge respectively. If the background electrons have a Maxwellian distribution, then $P_e = J_e(2\ kT_e/e)$, where J_e is the background electron current density. Substituting the experimental values, equation (1) becomes

$$12.05 + 35.5\, J_p + 11\, J_e = 21.95\ W/cm^2 \qquad (3)$$

Since the grid is floating,

$$J_p + J_e = J_i = 0.305\ A/cm^2 \qquad (4)$$

Equations (3) and (4) together give $J_p = 268\ mA/cm^2$ and $J_e = 37\ mA/cm^2$. Thus approximately 88% of the electron current collected by the floating grid are primaries.

IV. PLASMA PARAMETERS AND PROFILES

The cubical multiline-cusp source is normally operated in a 0.6 sec pulsed mode with density higher than 10^{12} ions/cm^3. The density and potential profiles and the electron temperature of the source plasma have been studied in detail by using the horizontal and axial Langmuir probes. A fast probe sweeping circuit has been developed [9] so that plasma can be sampled at any time during a discharge pulse, and also to prevent the probe from being destroyed by the high electron current. This sweeper completes a probe trace in 1.4 msec and has a maximum probe current capability of 5 A.

A plot of the electron temperature T_e and plasma potential V_p as a function of the discharge current I_d for the case when the plasma grid is connected to the negative cathode is shown in Fig. 5. This data is obtained with the Langmuir probe located at 14 cm from the grid and at a neutral pressure of 5×10^{-3} Torr. When I_d is increased from 50 to 475 A, V_p increases from 0.5 to 1.6 V above the anode potential while T_e increases from 2.8 to 6 eV. Figure 6 shows a similar behavior of V_p and T_e when the plasma grid is floating.

An axial profile of the plasma density is shown in Fig. 7 with V_d = 60 V and I_d = 560 A and the grid connected to the negative cathode. The profile is neither uniform nor symmetrical and is always sloping down towards the plasma grid. The density at the highest point is approximately 4×10^{12} ions/cm^3.

The axial potential profile has a similar appearance as the density profile. The data of Fig. 8 shows two distinct features: first, in the region within 6 cm from the grid, the potential of the plasma is negative with respect to the anode. Here, the rate of ion loss to the line cusps may be different from the region in

which V_p is positive relative to the anode. Secondly, since V_p is not uniform in the axial direction, an axial E field is present. The magnitude of this E field increases rapidly as one approaches the grid. Depending on the direction of the magnetic dipole-field, plasma will drift (the E x B drift) towards or away from the chamber wall. If the source chamber is cylindrical in geometry, then the pattern created by the plasma on the grid always shows only half the number of cusps. In the magnet arrangement of Fig. 2b, plasma drifts away from the wall in two of the opposite corners and drifts inward in the other two. Thus the uniform region of one diagonal direction is smaller than that of the other.

A uniform density profile across the extraction area of an ion source is essential for good beam optics. Movable Langmuir probes installed about 2 mm from the grid are used to scan the profile in the horizontal and diagonal directions. These probes are biased at -22.5 V relative to the cathode to collect ion saturation current. Figures 9 and 10 are typical horizontal and diagonal profiles obtained at a neutral pressure of 5×10^{-3} Torr. Uniformity of the density is better than 4% within a region of 10 x 10 cm. From these profile measurements, it is also found that the position where the uniformity breaks corresponds approximately to the boundary where the energetic primary electrons can penetrate. As the discharge voltage V_d (and therefore the energy of the primaries) is varied, the breaking point of the profile is found to shift accordingly.

When the neutral pressure is increased to 8×10^{-3} Torr, the horizontal profile becomes non-uniform as illustrated in Fig. 11. The ionization mean free path ($\sim$35 cm) is now nearly equal to the length of the chamber. As a result, plasma generation is no longer uniform throughout the extraction region, but is localized around the filaments. In spite of the fact that the pressure is increased from 5×10^{-3} to 8×10^{-3} Torr, there is no significant change in

the current density J_i at the center of the grid for I_d between 50 to 600 A (Fig. 12). These results indicate that it is not favorable to operate this multiline-cusp source at a neutral pressure higher than 5×10^{-3} Torr.

The discharge (arc) efficiency is defined as the ratio of the total ion current collected at the extraction area of the plasma grid to the discharge power. The deuterium ion current density J_i measured at the grid for V_d = 60, 70 and 80 V is shown in Fig. 13 as a function of I_d for the case when the grid is connected to the negative cathode. If an extraction region 14 x 14 cm is assumed, (i.e. allowing 5 cm from the wall), then the discharge efficiency for J_i = 300 mA/cm^2 is 2.1, 2.0 and 1.87 A/kW for V_d = 80, 70 and 60 V respectively. If the grid return current is included in I_d, then the above discharge efficiency becomes 1.75, 1.73 and 1.63 A/kW.

When hydrogen is used to generate the plasma in the source, it is found that J_i at the grid is different from that of deuterium for the same discharge power and gas pressure. Fig. 14 shows that J_i at the grid for hydrogen is generally 12% higher than that of deuterium. Hydrogen and deuterium have almost identical cross-sections for ionization by electrons [10], and therefore the ion production rate for both plasmas should be equal for the same neutral density. However, because of the difference in mass between these two isotopes, the ion loss rate at the cusps, the electron temperature and the plasma density are different and so will lead to the difference in J_i.

V. DISCHARGE CHARACTERISTICS

Hair-pin tungsten filaments (0.15 cm diam) have been used as cathodes for the multiline-cusp source in 0.6 sec pulse operations. Fig. 15 is an oscilloscope display of the discharge voltage V_d, the discharge current I_d and the ion saturation probe current I_p. Once the discharge is pulsed on, V_d rises rapidly to 80 V and then gradually decays to 63 V in 0.1 sec. On the other hand, I_d starts approximately from 200 A and then increases to 340 A in the same time interval. This discharge characteristic indicates that the filaments are operated in the emission-limited regime during the early part of the pulse. However, the temperature of the filament will gradually increase in the later part of the pulse due to additional heating by ion bombardment. As a result, the filaments eventually operate in a more space-charge limited condition.

Spring shape non-inductive tungsten filaments (0.15 cm diam) have also been tested in this source. For reasons not yet well understood, it is found that if this kind of filament becomes too hot and arrives at or near the space-charge limited condition, the discharge mode changes to one in which the plasma potential is well below the anode potential. This new mode is characterized by a high discharge voltage, a low discharge current and a low density plasma with a higher noise level. In order to avoid this inefficient discharge mode, one must lower the filament temperature so that the filaments are operated more emission-limited. It happens occasionally that these filaments are operated at the boundary of space-charge and emission-limited regimes. Since they can either be heated or cooled in time (depending on whether the electron emission cooling or the ion bombardment heating prevails), the unusual mode-flipping phenomenon can occur during a discharge pulse.

When the source is operated with a long pulse duration (∿1.5 sec), tungsten filaments may no longer be useful as cathodes because of their short lifetime. For this reason, lanthanum hexaboride and impregnated oxide emitters are being investigated as alternate cathodes for the multiline-cusp source. Fig. 16 shows a 2.5 cm diam and 3.0 cm long cylindrical impregnated oxide cathode, which is mounted on a molybdenum holder. This cathode is heated internally by a non-inductive tungsten filament. After the discharge is turned on, the external surface of the cathode will receive additional heating from the plasma. Mode-flipping is also found to occur quite frequently when the source is operated with these magnetic-field-free cathodes. Fig. 17A shows how the discharge changes from an efficient into an inefficient mode during a 3.0 sec discharge pulse. If one column of magnets is removed from the end plate of the source chamber (thus creating a larger anode area), the second mode disappears as shown in Fig. 17B. This result suggests that the mode-flipping phenomenon is also related to the anode area of the source. A detailed study of these new cathodes is in progress and results will be reported.

VI. ION SPECIES MEASUREMENT

A hydrogen or a deuterium ion source always contains atomic and molecular ion species. To increase plasma penetration by neutral beam, a high percentage of H^+ or D^+ is desired. The species composition has been investigated for two cylindrical multiline-cusp sources (diam = 20 cm, length = 14 and 25.5 cm) that are operated in a dc mode. A low energy ($\sim$300 eV) hydrogen beam was extracted from these sources by a three grid accel-decel system. The beam was analyzed by a 180^o magnetic deflection mass spectrometer [11]. Figure 18 shows the species percentage of the two sources when the discharge voltage V_d is 60 V and the discharge current I_d is varied from 2 to 28 A. The ion current density J_i at the plasma grid is also presented in the same diagram. Results of the measurement can be summarized as follows: (1) For the same I_d, and therefore the same discharge power, both the long and short sources produce the same percentage of H^+, but the current density J_i at the plasma grid of the short source is about 35% higher than that of the long source. (2) The beam of the longer source generally contains a higher percentage of H_3^+. (3) As I_d is increased, the percentage of H^+ goes up while H_3^+ decreases. However, the percentage of H_2^+ remains approximately constant. When the percentage of H_3^+ gradually falls below 10%, it is expected that any further increase of H^+ will be accompanied by a decrease in H_2^+. The 24 cm cubical multiline-cusp source has been operated with I_d = 650 A, other diagnostic techniques have shown that the percentage of H^+ in a 110 keV beam reaches approximately 80% [12].

ACKNOWLEDGMENTS

We would like to thank M. D. Williams for all the technical assistance and members of the Berkeley neutral beam group for valuable discussions. The skillful technical work of L. A. Biagi, H. H. Hughes. and members of their group is also gratefully acknowledged.

This work is supported by the U. S. Department of Energy. Office of Fusion Energy, under contract No. W-7405-ENG-48.

REFERENCES

1. PLT GROUP, paper C3 presented at the 7th International Conference on Plasma Physics and Controlled Nuclear Fusion Research, Innsbruck, Austria (1978).

2. R. LIMPAECHER and K. R. MACKENZIE, Rev. Sci. Instrum., 44, (1973) 726.

3. Plasma Physics and Fusion Progress Report, Culham Lab. Rep. CLM-PR 20, (1978).

4. W. L. STIRLING, P. M. RYAN, C. C. TSAI, and K. N. LEUNG, Rev. Sci. Instrum., 50, (1979) 102.

5. K. N. LEUNG, T. K. SAMEC, and A. LAMM, Phys. Lett. A51, (1975) 490.

6. K. W. EHLERS and K. N. LEUNG, Rev. Sci. Instrum., 50, (1979) 356.

7. K. N. LEUNG, R. D. COLLIER, L. B. MARSHALL, T. N. GALLAHER, W. H. INGHAM, et al., Rev. Sci. Instrum., 49, (1978) 321.

8. J. R. TREGLIO and J. A. PATERSON, Bull. Am. Phys. Soc., 23, (1978) 747.

9. K. A. MILNES, K. W. EHLERS, K. N. LEUNG, and M. D. WILLIAMS, Lawrence Berkeley Lab. Report, LBL-8605 (1979).

10. C. R. BARNETT, et al., "Atomic Data for Controlled Fusion Research," ORNL-5207, p. C. 4.8 (1977).

11. K. W. EHLERS, K. N. LEUNG, and M. D. WILLIAMS, Lawrence Berkeley Lab. Report, LBL-8863 (1979).

12. C. F. BURRELL, J. W. STEARNS and R. R. SMITH, private communications.

FIGURE CAPTIONS

Fig. 1 Schematic diagram of the multiline-cusp ion source.

Fig. 2 The two full-line cusp magnet arrangement on the source chamber.

Fig. 3 Ion current density near the plasma grid as a function of the discharge current at 70 V discharge voltage.

Fig. 4 Typical voltage signal recorded by the Norland 2001-A computer system.

Fig. 5 Electron temperature and plasma potential at the center of the source chamber as a function of the discharge current when the plasma grid is connected to the negative cathode. A typical Langmuir probe characteristic is also shown in the lower right hand corner.

Fig. 6 Electron temperature and plasma potential at the center of the source chamber as a function of the discharge current when the plasma grid is electrically floating.

Fig. 7 A typical axial plasma density profile.

Fig. 8 The axial plasma potential profile.

Fig. 9 A typical horizontal density profile near the plasma grid at a neutral pressure of 5×10^{-3} Torr.

Fig. 10 A typical diagonal density profile near the plasma grid at a neutral pressure of 5×10^{-3} Torr.

Fig. 11 The horizontal density profile near the plasma grid at a neutral pressure of 8×10^{-3} Torr.

Fig. 12 Ion current density near the plasma grid as a function of the discharge current for two different neutral pressures.

Fig. 13 Ion current density near the plasma grid as a function of the discharge current for V_d = 60, 70 and 80 V.

Fig. 14 Ion current density near the plasma grid as a function of the discharge current for hydrogen and deuterium plasmas at a neutral pressure of 5×10^{-3} Torr.

Fig. 15 Oscilloscope display of the discharge voltage, the discharge current and the ion saturation probe current with tungsten filaments as the cathode.

Fig. 16 A cylindrical impregnated oxide cathode.

Fig. 17 Oscilloscope display of the discharge voltage, the discharge current and the ion saturation probe current for the cylindrical impregnated oxide cathode (A) with, and (B) without mode flipping.

Fig. 18 The percentage of species current as a function of discharge current and ion current density near the plsma grid with discharge voltage 60 V.

Table I. Comparison of various parameters when the plasma grid is floating or connected to the negative cathode.

Grid connected to negative cathode	Grid floating
V_d = 67.5 V	V_d = 75 V
I_d = 450 A	I_d = 510 A
I_g = 84 A	V_{float} = 35.5 V
P_d = (67.5)(450 + 84) = 36.1 kW	P_d = (75 V)(510 A) = 38.25 kW
P_h^t = 206 (Arb. unit)	P_h^f = 216 (Arb. unit)
J_i = 310 mA/cm^2	J_i = 305 mA/cm^2
P_t = (310)(67.5) = 20.93 W/cm^2	$P_f = P_t(P_h^f / P_h^t)$ = 21.95 W/cm^2

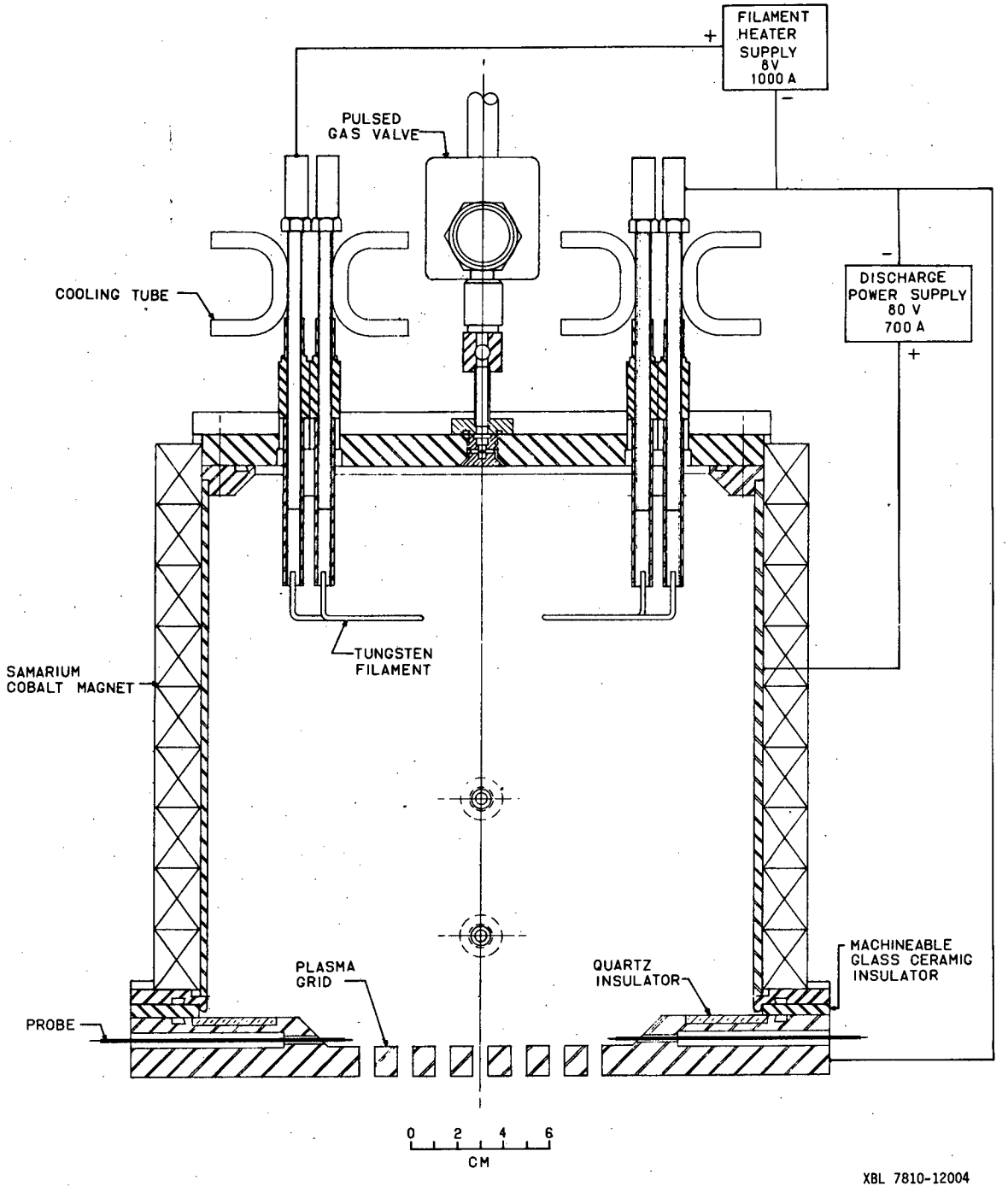
FILAMENT
HEATER
SUPPLY
8V
1000 A
+
−
PULSED
GAS VALVE
COOLING TUBE
DISCHARGE
POWER SUPPLY
80 V
700 A
−
+
TUNGSTEN
FILAMENT
SAMARIUM
COBALT MAGNET
PLASMA
GRID
QUARTZ
INSULATOR
MACHINEABLE
GLASS CERAMIC
INSULATOR
PROBE
0 2 4 6
CM
XBL 7810-12004

Fig. 1

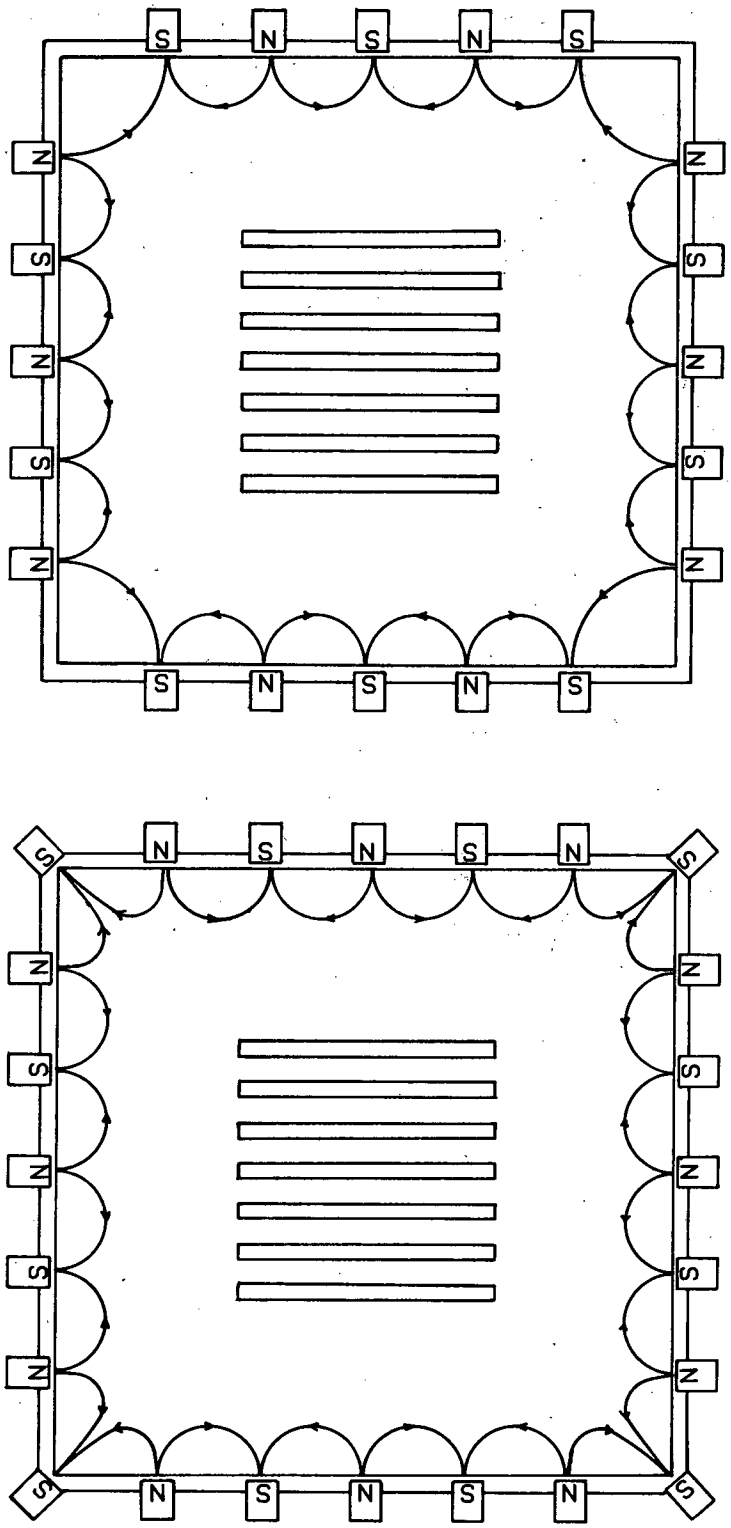

XBL 791-7722

Fig. 2

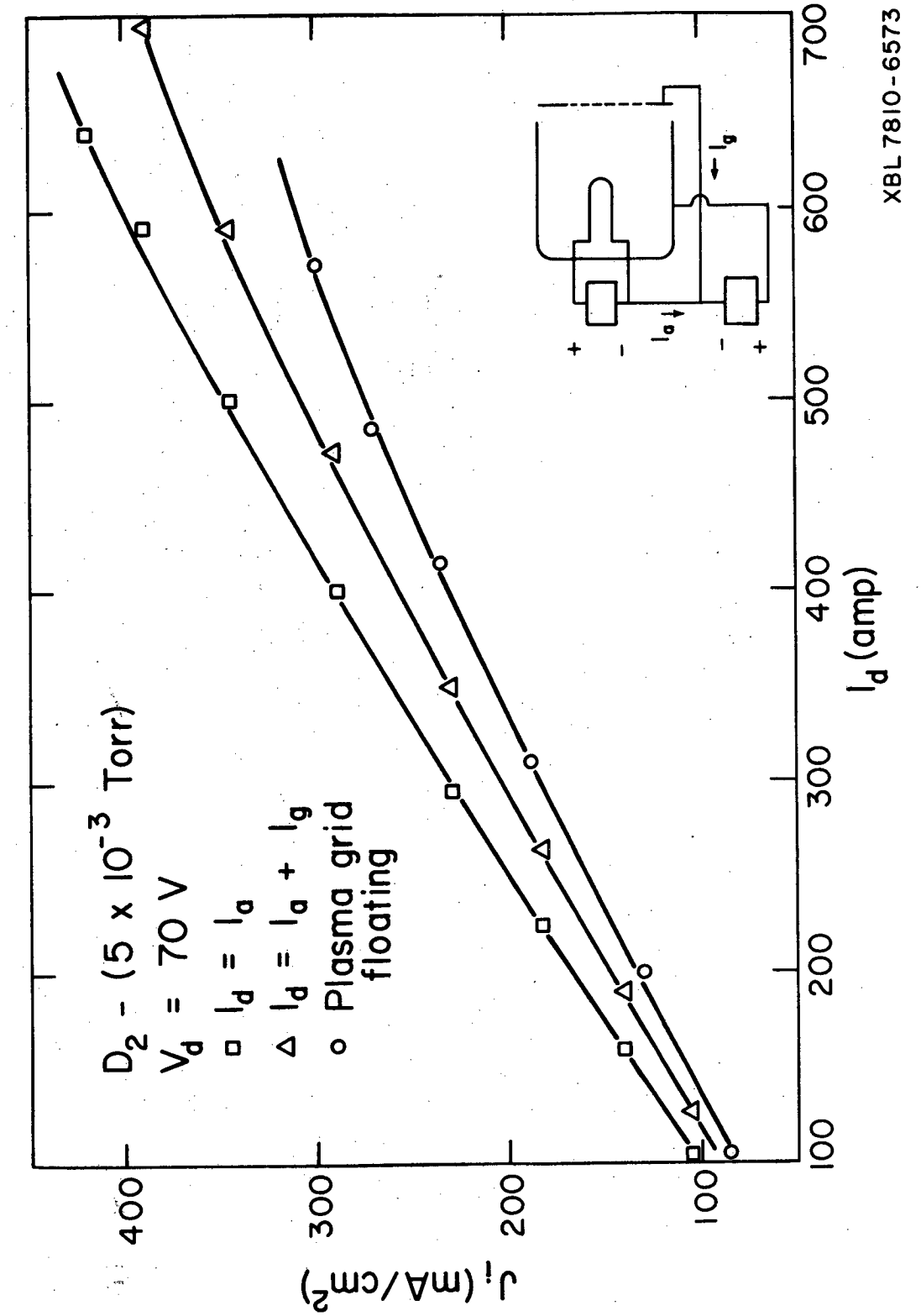
D_2 - (5 x 10^{-3} Torr)
V_d = 70 V
□ $I_d = I_a$
△ $I_d = I_a + I_g$
○ Plasma grid floating
j_i (mA/cm^2)
I_d (amp)
100
200
300
400
500
600
700
I_a
I_g
+
−
−
+
XBL 7810-6573

Fig. 3

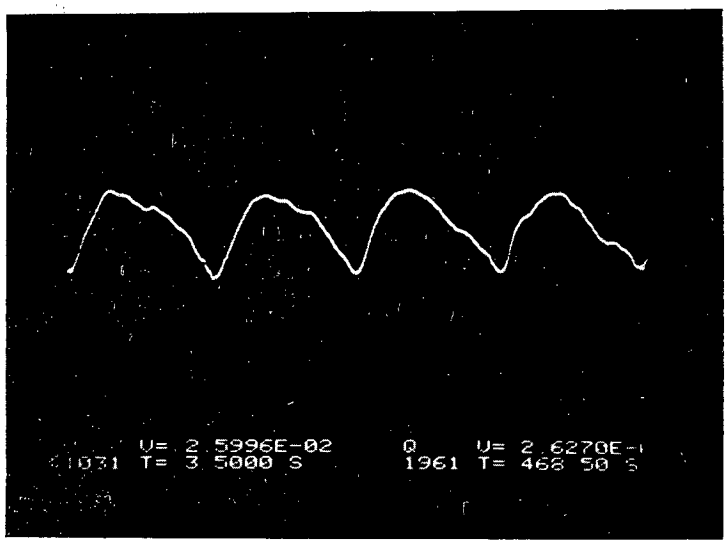

XBB 791-215

Fig. 4

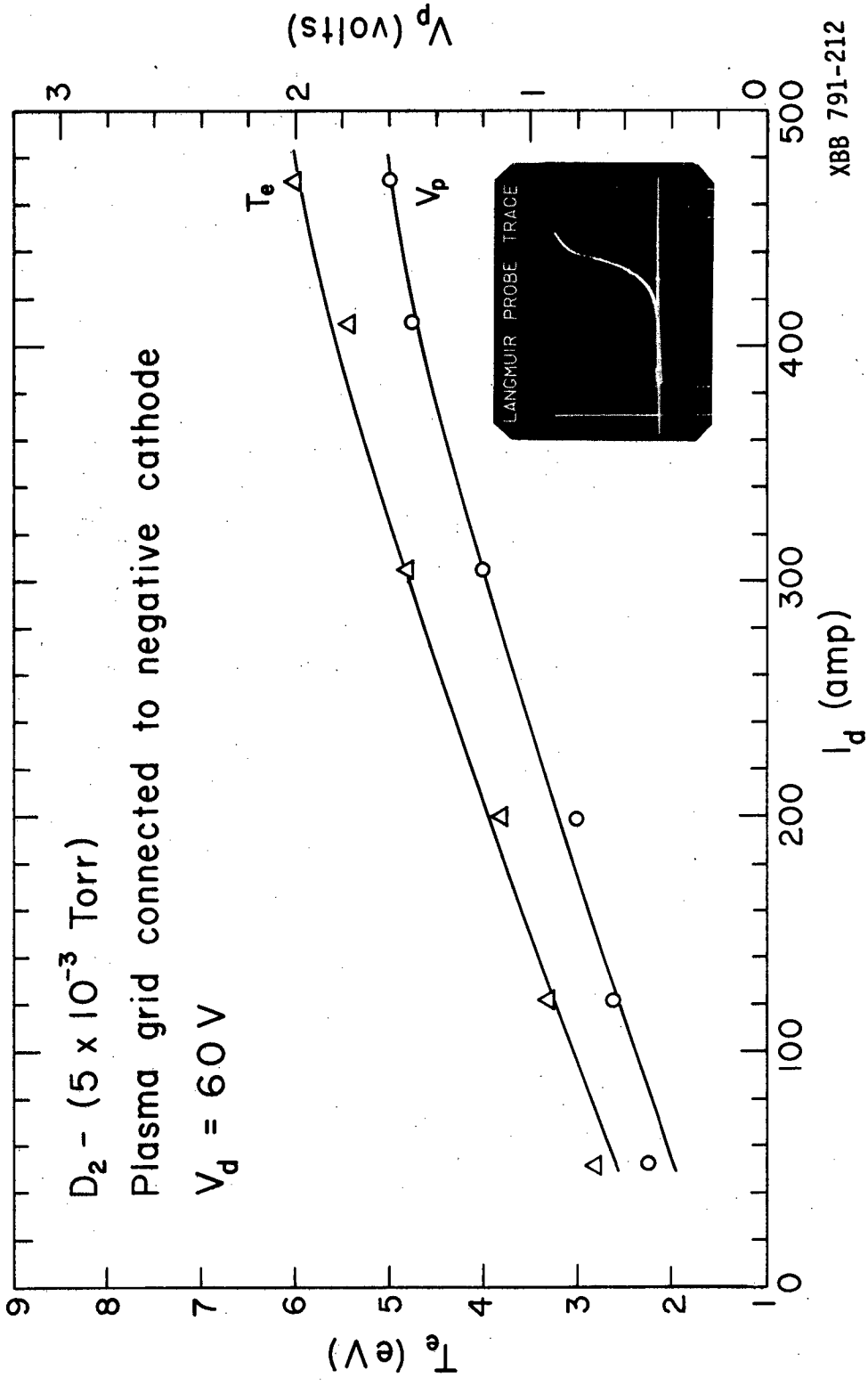
V_p (volts)
T_e (eV)
I_d (amp)
T_e
V_p
D_2 - (5×10^{-3} Torr)
Plasma grid connected to negative cathode
V_d = 60 V
LANGMUIR PROBE TRACE
XBB 791-212

Fig. 5

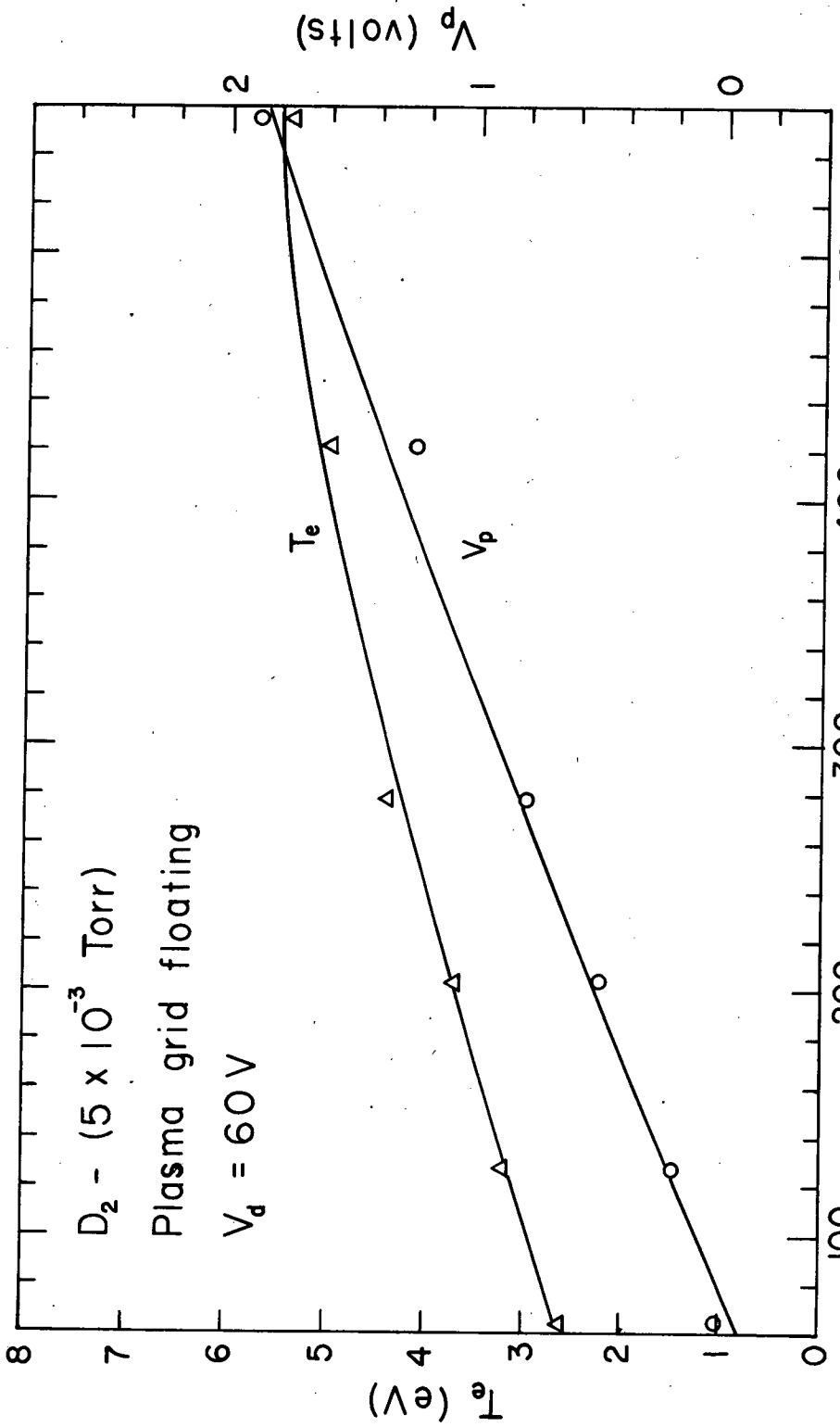

XBL 791-7724

Fig. 6

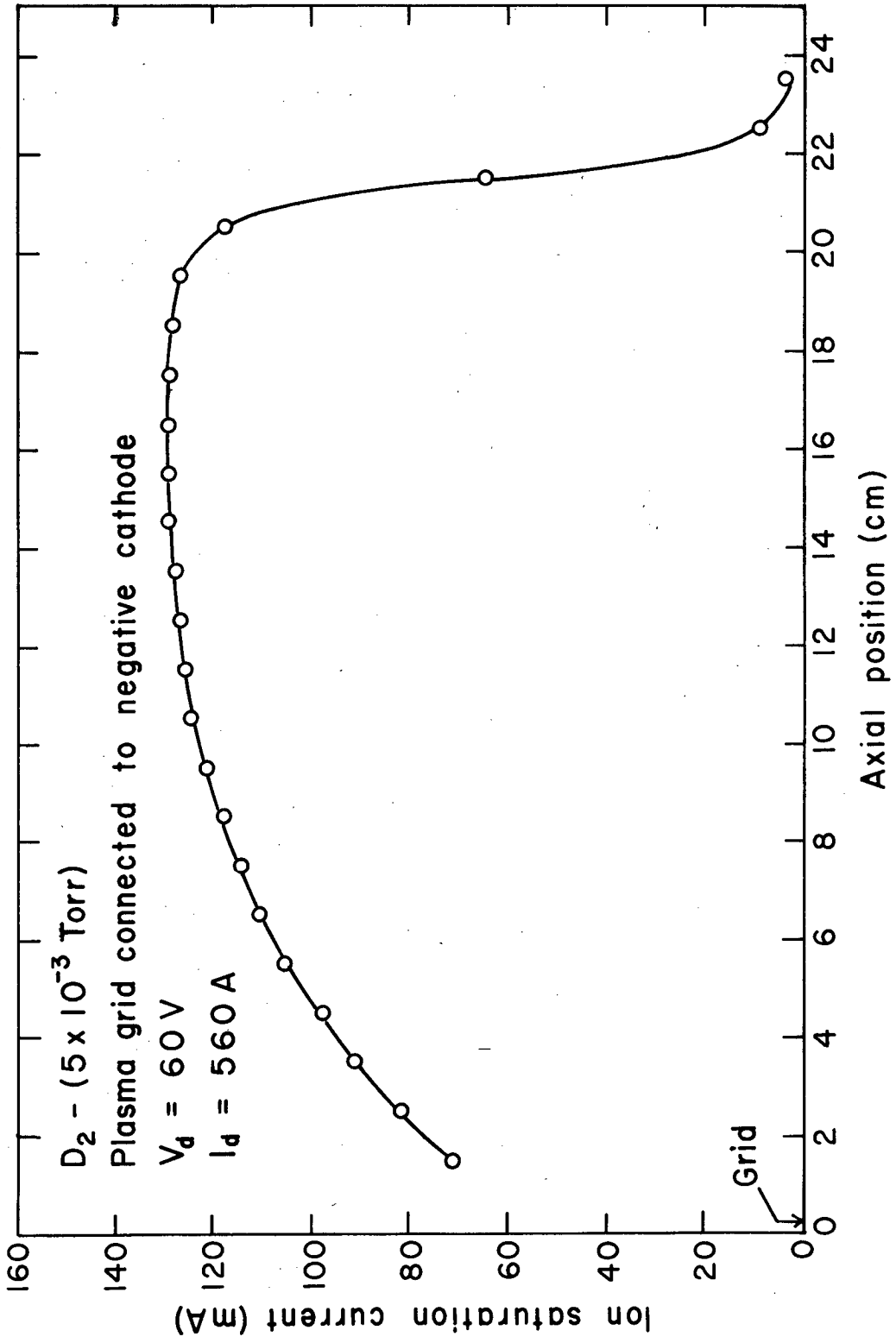

XBL 791-7725

Fig. 7

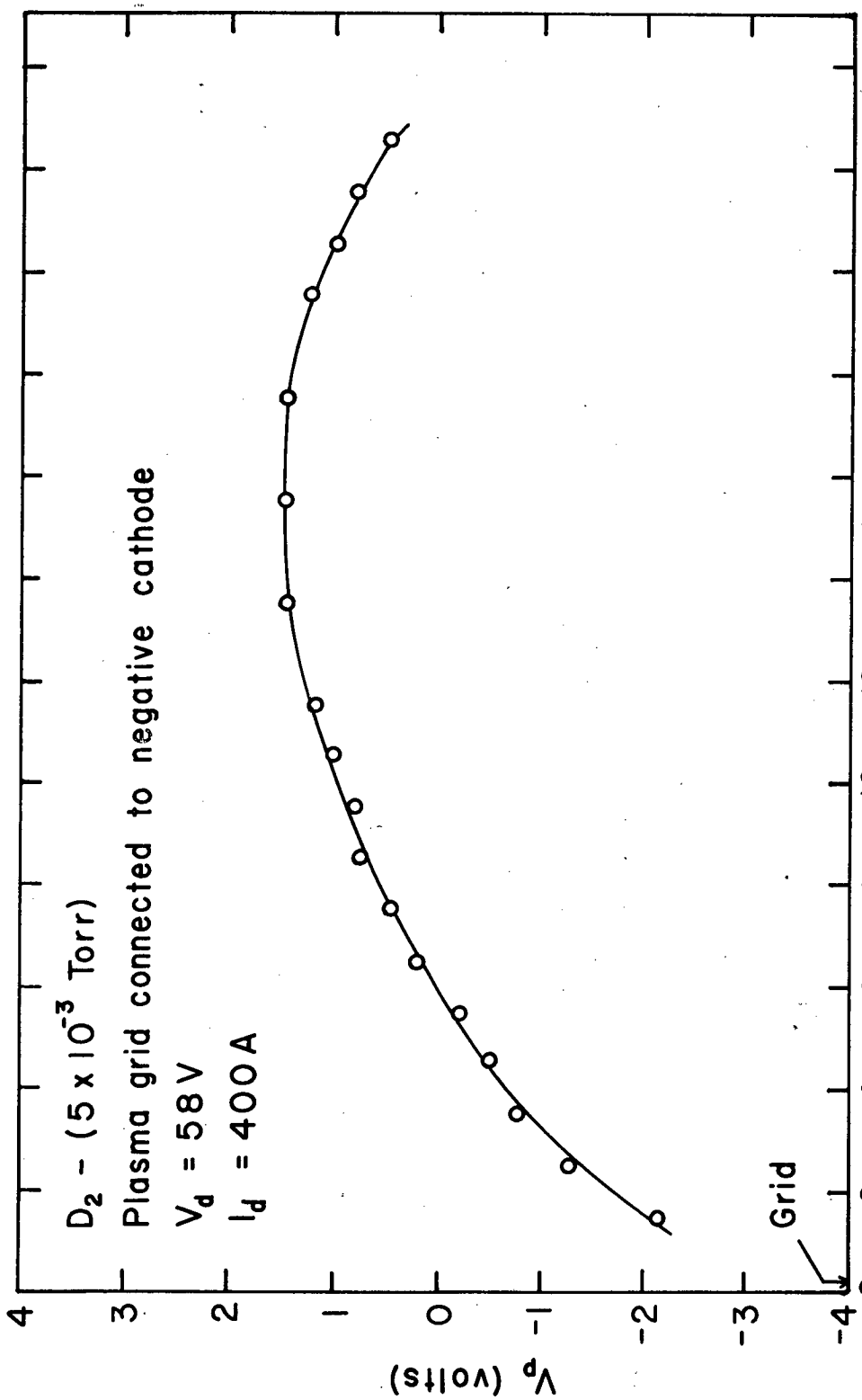

XBL 791-7726

Fig. 8

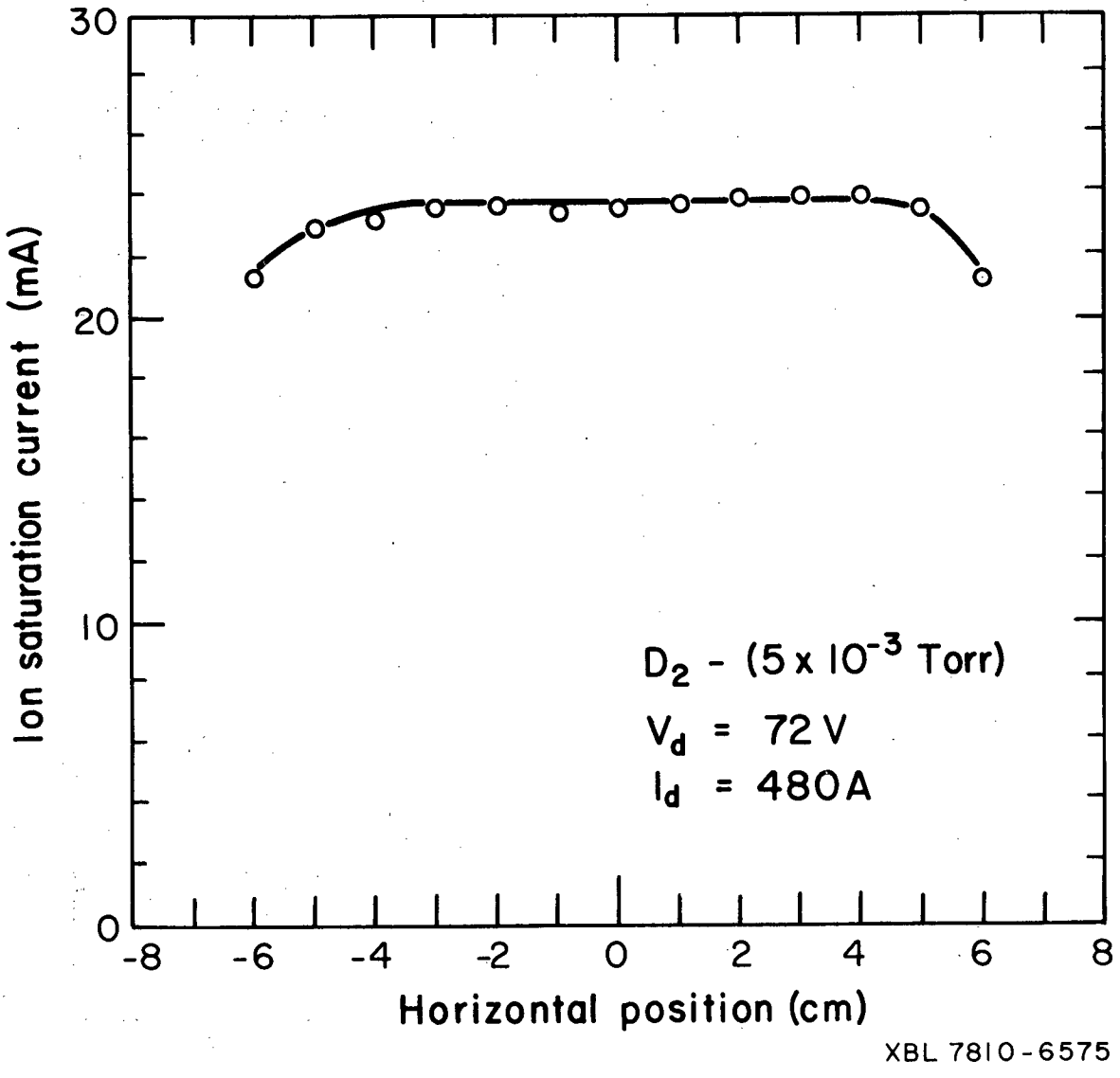
30
20
10
0
Ion saturation current (mA)
-8
-6
-4
-2
0
2
4
6
8
Horizontal position (cm)
D_2 - (5×10^{-3} Torr)
V_d = 72 V
I_d = 480A
XBL 7810-6575

Fig. 9

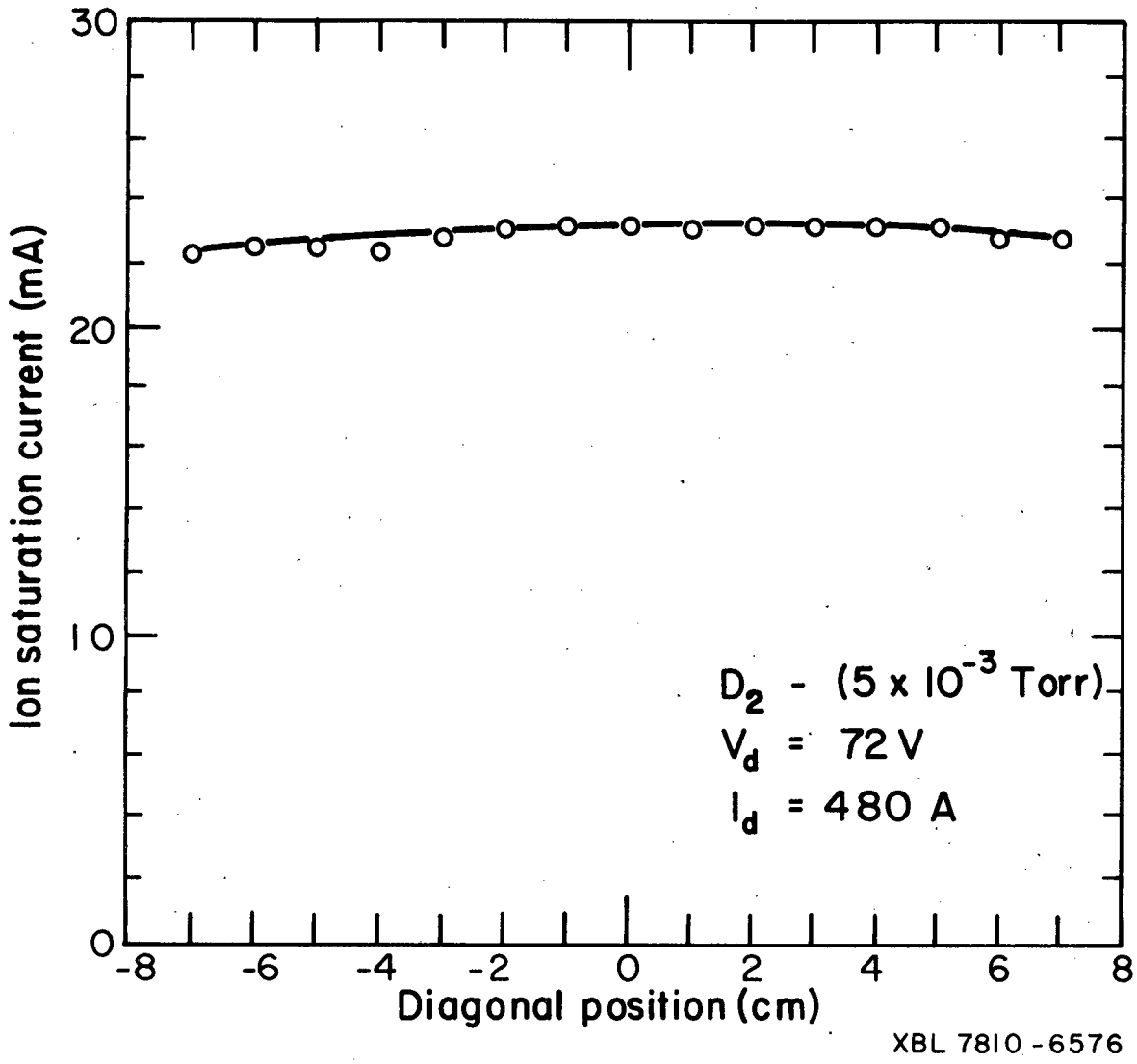
30
20
10
0
Ion saturation current (mA)
-8
-6
-4
-2
0
2
4
6
8
Diagonal position (cm)
D_2 - (5 x 10^{-3} Torr)
V_d = 72 V
I_d = 480 A
XBL 7810-6576

Fig. 10

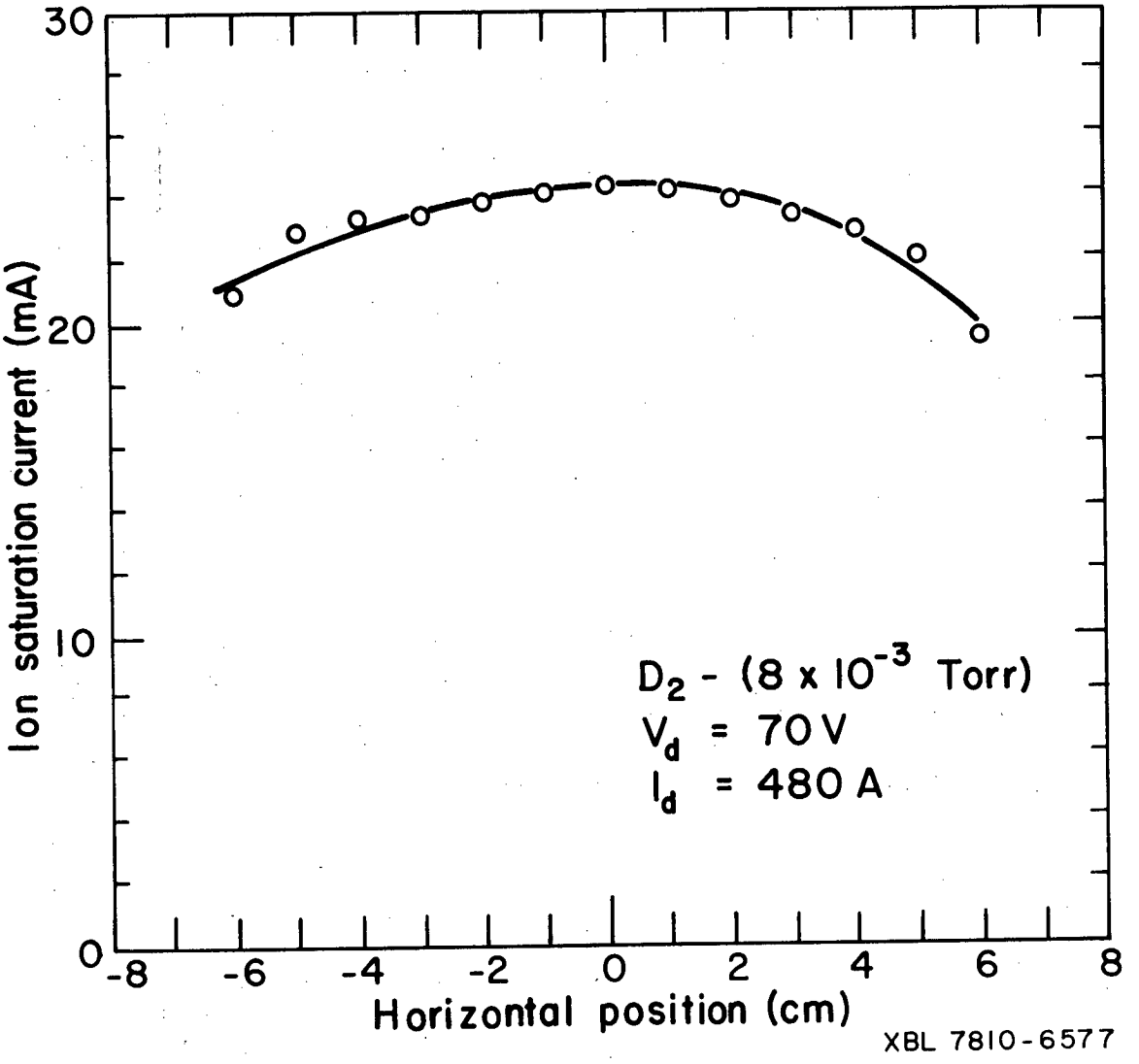
30
20
10
0
Ion saturation current (mA)
-8
-6
-4
-2
0
2
4
6
8
Horizontal position (cm)
D_2 - (8×10^{-3} Torr)
V_d = 70 V
I_d = 480 A
XBL 7810-6577

Fig. 11

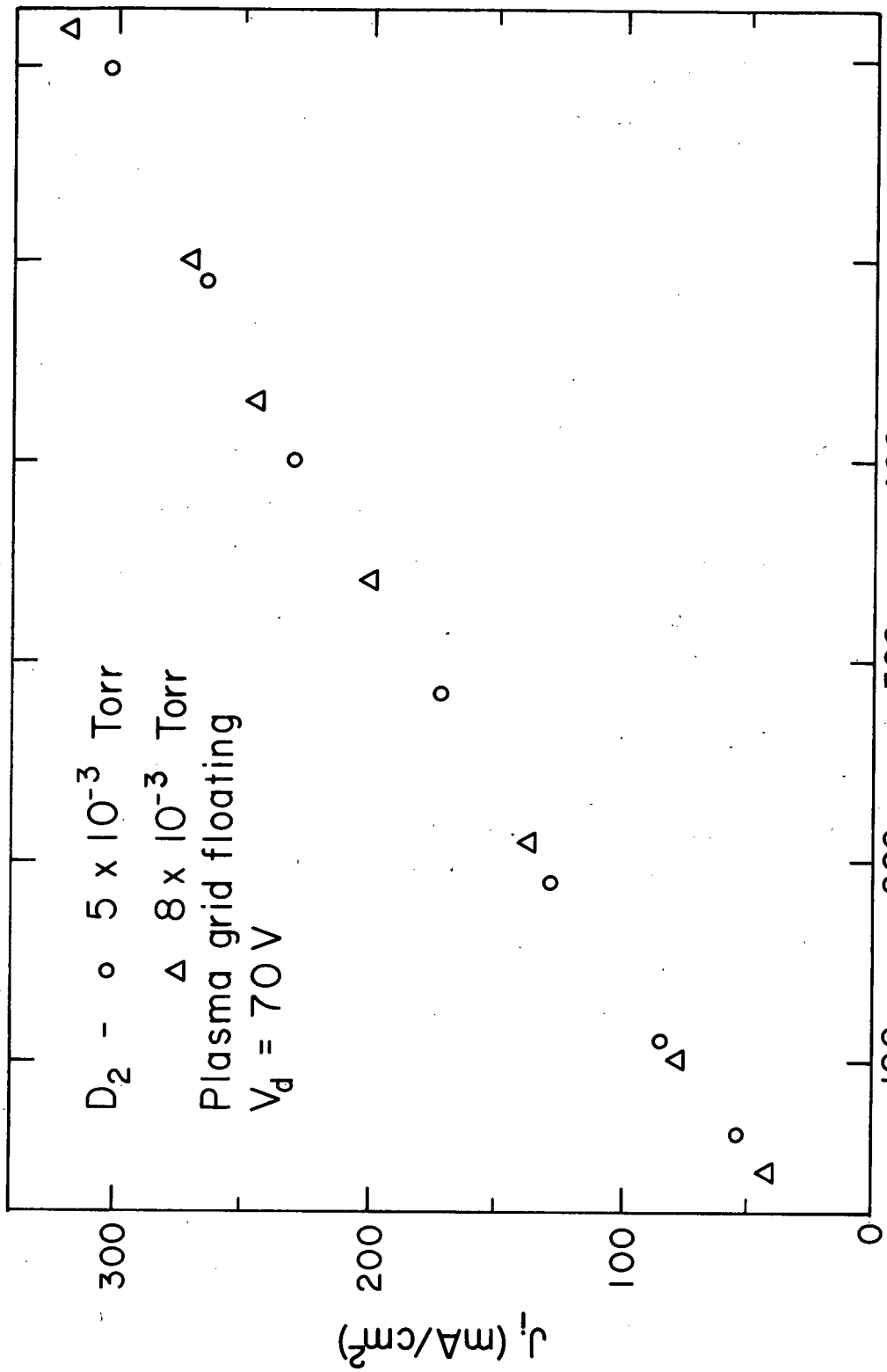

XBL 7810-6572

Fig. 12

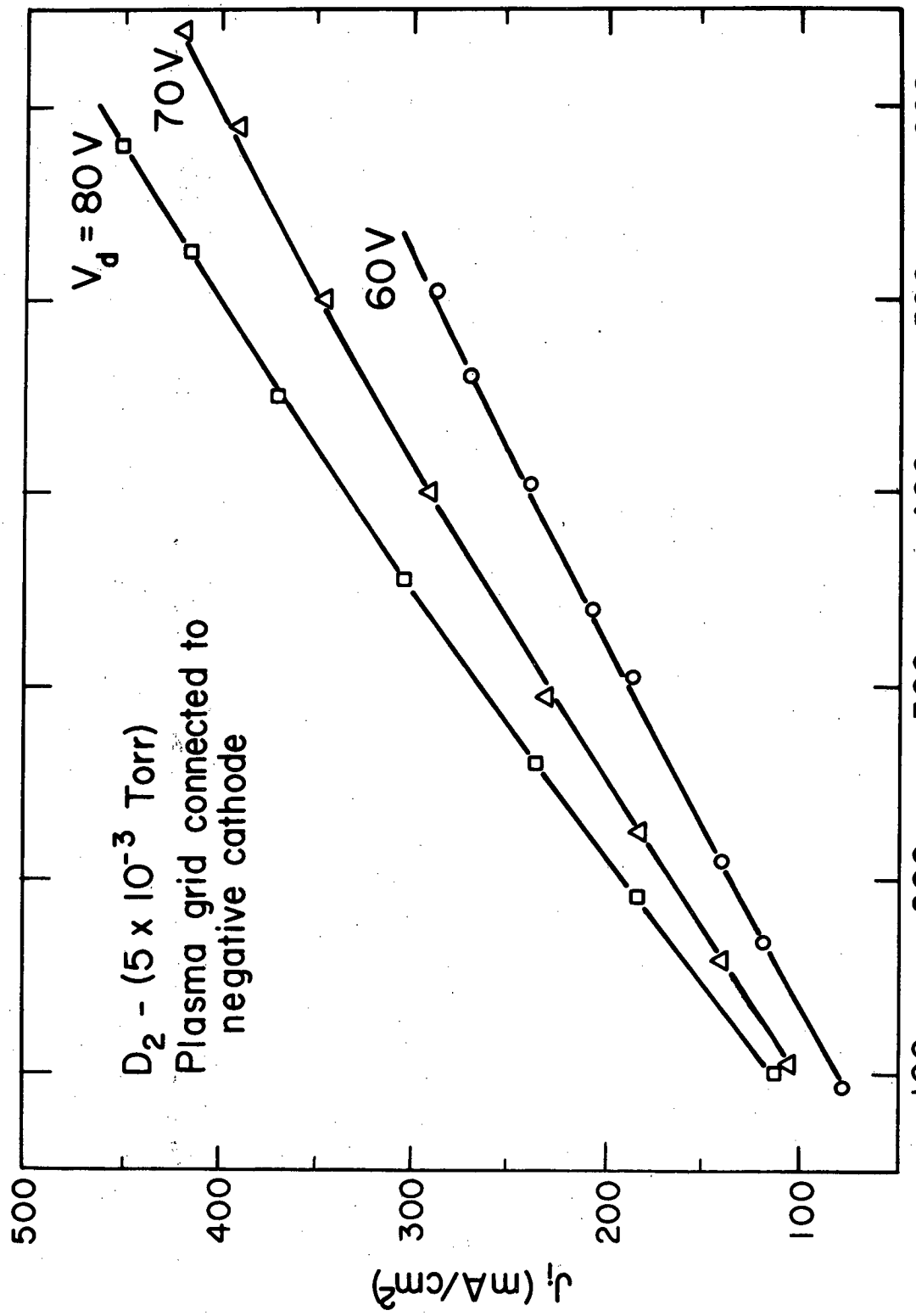
V_d = 80 V
70 V
60 V
D_2 - (5 x 10^{-3} Torr)
Plasma grid connected to
negative cathode
j_i (mA/cm^2)
I_d (amp)
100
200
300
400
500
600
XBL 7810-6574

Fig. 13

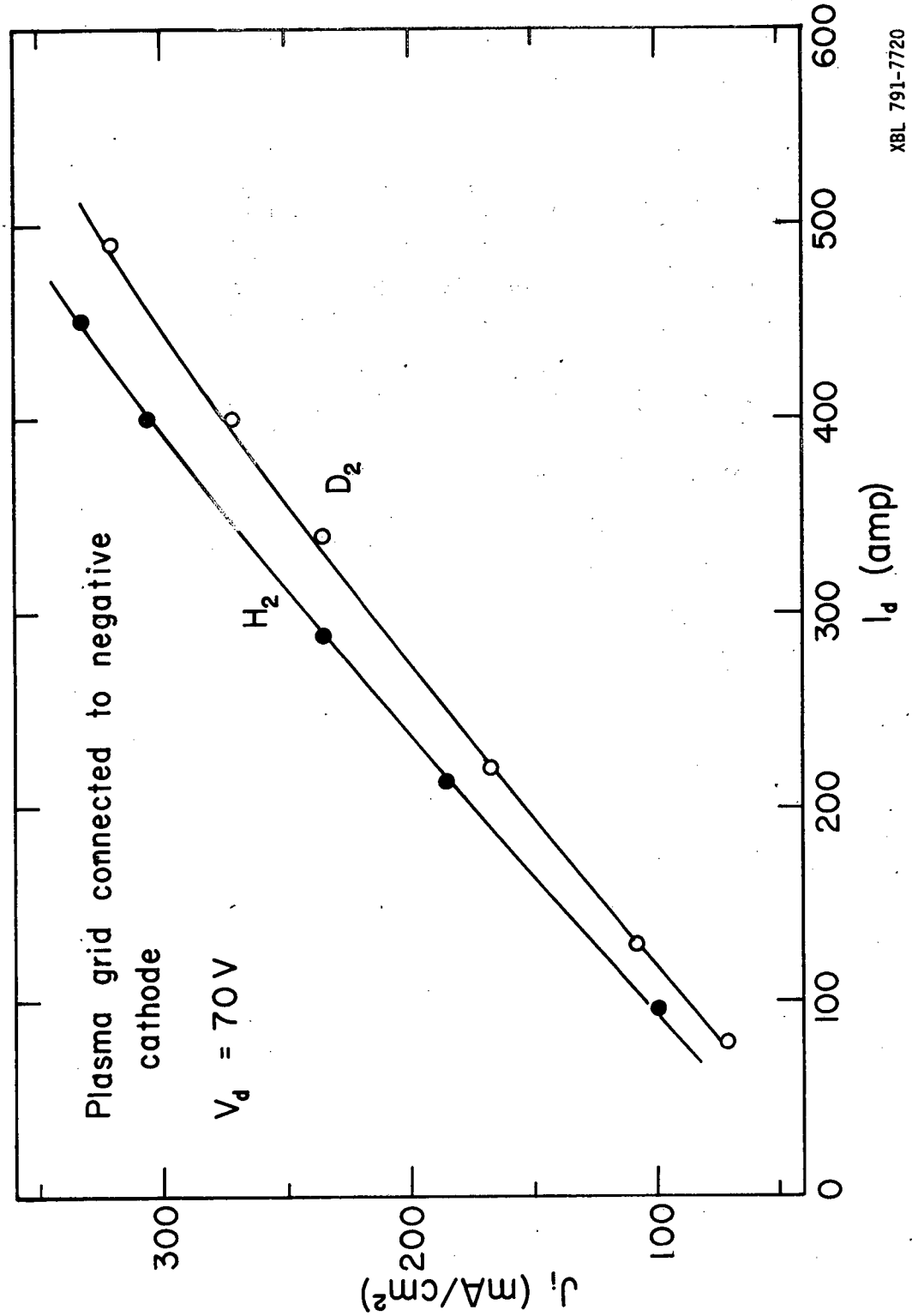

XBL 791-7720

Fig. 14

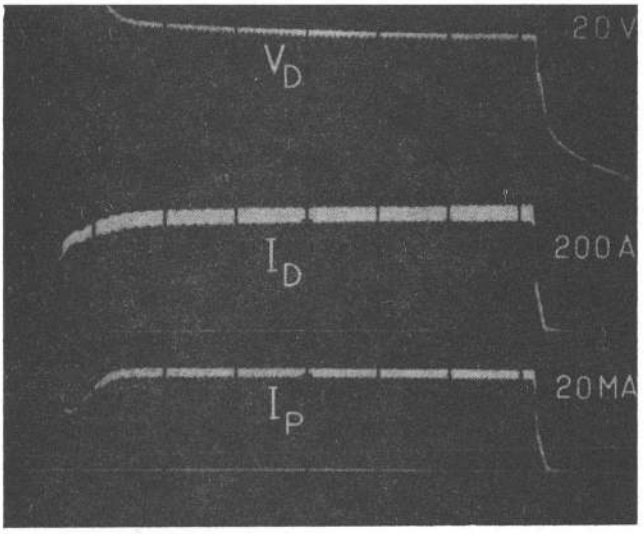

XBB 793-4012

0·1 SEC/DIV.

Fig. 15

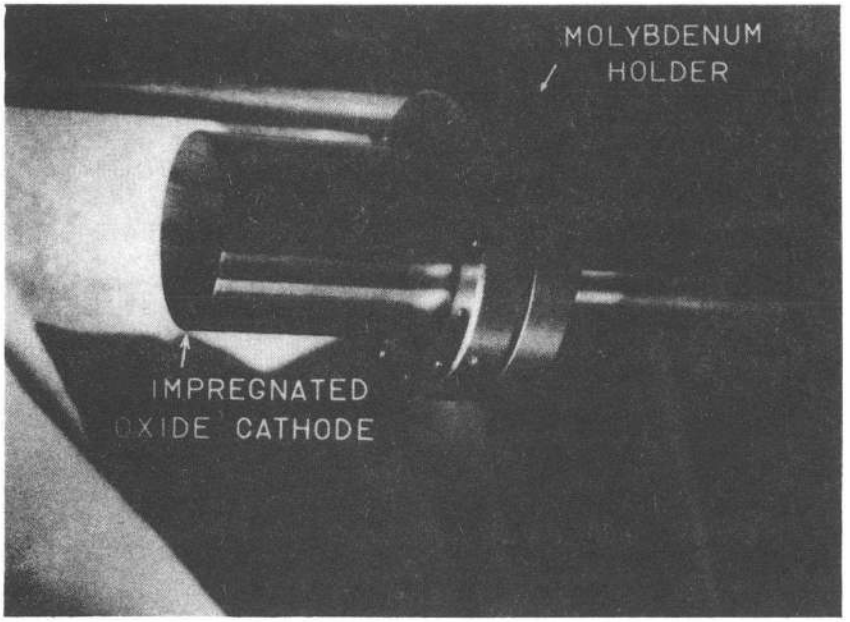

XBB 793-4013

Fig. 16

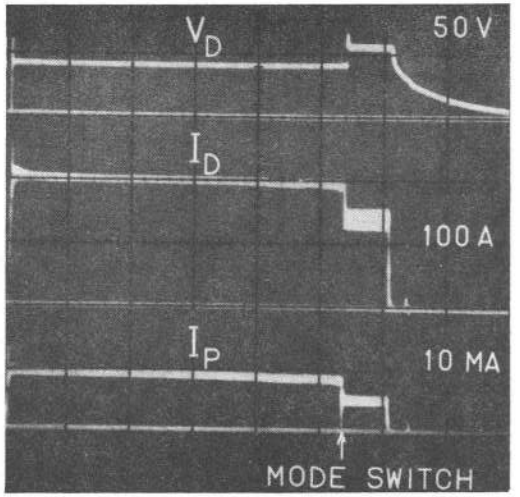

0·5 SEC/DIV.

(A)

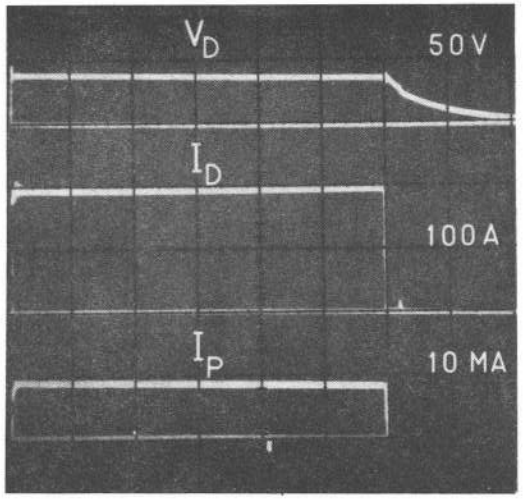

0·5 SEC/DIV.

(B)

XBB 793-4011

Fig. 17

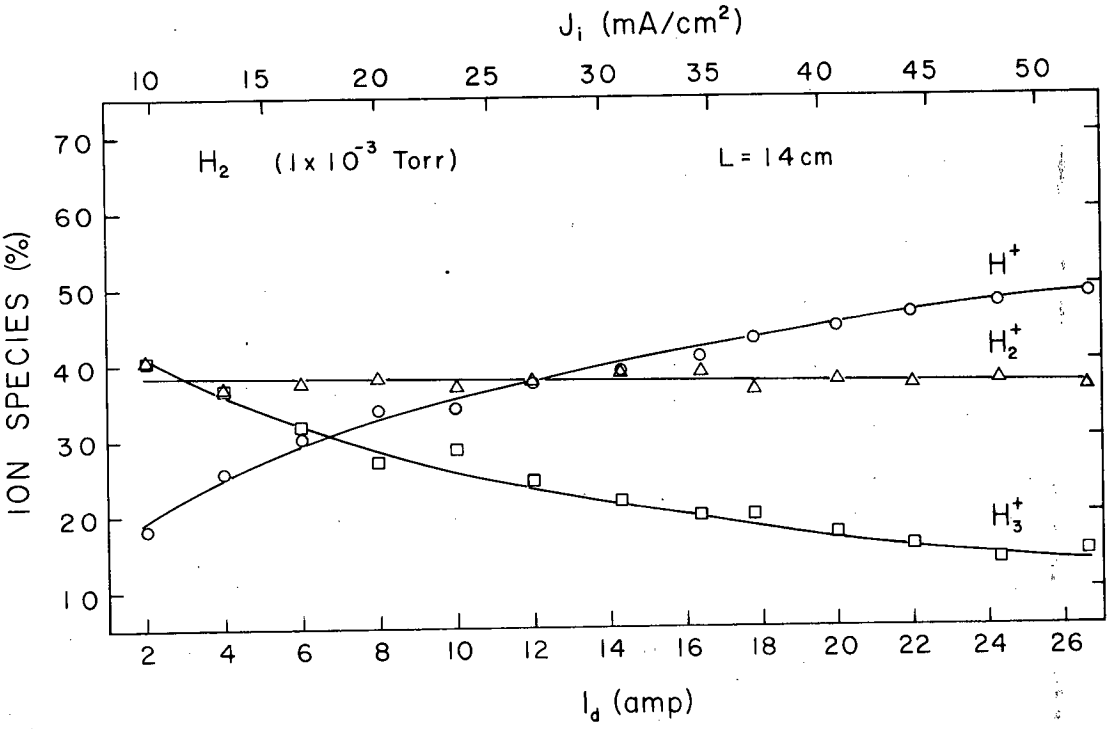

(A)

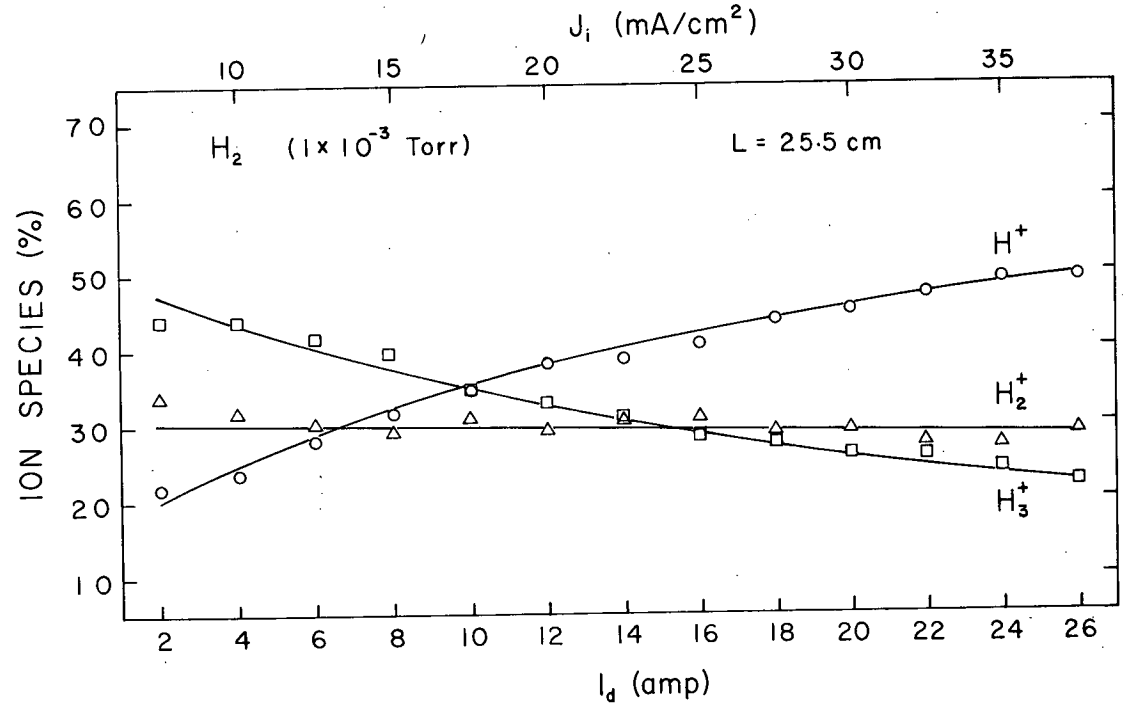

(B)

XBL 792-8649

Fig. 18

TECHNICAL INFORMATION DEPARTMENT
LAWRENCE BERKELEY LABORATORY
UNIVERSITY OF CALIFORNIA
BERKELEY, CALIFORNIA 94720